J Mater Sci: Mater Electron (2022) 33:3465–3484

Flexible and stretchable strain sensors fabricated by inkjet printing of silver nanowire-ecoflex composites

R. Madhavan[1,*]

[1] *Department of Chemical Engineering, Indian Institute of Science, Bengaluru 560012, Karnataka, India*

Received: 3 September 2021
Accepted: 5 December 2021
Published online: 22 January 2022

© The Author(s), under exclusive licence to Springer Science+Business Media, LLC, part of Springer Nature 2021

ABSTRACT

Recently, the fabrication of strain sensors with high sensitivity and high stretchability, which can precisely monitor subtle strains and large mechanical deformations exhibited by the human bodily motions, is critical for healthcare, human–machine interfaces, and biomedical electronics. However, a great challenge still exists i.e. achieving strain sensors with both high sensitivity and high stretchability by a facile, low-cost and scalable fabrication technique. Herein, this work reports Silver nanowires (AgNWs)/Ecoflex based composite strain sensors via inkjet printing technique which precisely deposits functional materials in a rapid, non-contact and maskless approach allowing high volume production. Noteworthily, the fabricated strain sensor display many fascinating features, including high sensitivity (a gauge factor of 13.7), a broad strain sensing range over 30%, excellent stability and reliability (>1000 cycles), and low monitoring limit (<5% strain). These remarkable features allow the strain sensor to effectively monitor various human motions. This work opens up a new path for fabricating nanocomposite thin film-based strain sensors for wearable electronics.

1 Introduction

Nowadays, the flexible/stretchable, wearable and skin mountable strain sensors are attracting much attention as they convert external strains or deformations into electrical signals and are widely employed for detecting human motion [1, 2], metabolic rate [3], muscle movement [4–6], and rehabilitation of disabled persons [7, 8]. In recent years, monitoring of human motions has drawn significant research attention for the development of bionic ligaments [9], artificial intelligence [10] and other electronic devices for healthcare related applications [11, 12]. For monitoring of human motions, the strain sensors should exhibit desirable characteristics such as mechanical flexibility, stretchability, sensitivity, long-term durability and detection of static as well as dynamic mechanical deformations [13, 14]. Traditional strain sensors exhibit rigidity and exhibit detection of minute strain (less than 5%) [15, 16]. On the other hand, flexible/stretchable strain sensor can sustain large-scale mechanical strains [17–20]. There are various types of stretchable and wearable strain sensors including resistive-type [21], resistive-

Address correspondence to E-mail: madhavan_rajaa@rediffmail.com

https://doi.org/10.1007/s10854-021-07540-8

capacitive integrated sensors [22], piezotronic sensors [23], and so on. Among them, resistive-type strain sensors with broad strain sensing range and high sensitivity are highly desirable due to their ease of fabrication, simple device structures and readout methods [24, 25]. Moreover, resistive-type strain sensors in the form of composites have attracted much attention owing to their ability to combine active sensor material and the flexible/stretchable supporting material in order to achieve remarkable functional properties and sensing performance and are promising candidates for wearable and skin mountable strain sensors. [26, 27].

The critical sensing parameter of flexible/stretchable resistive-type strain sensors is sensitivity or gauge factor (GF) which is evaluated by the ratio of relative resistance variation $\Delta R/R_0$ to the applied tensile strain ε ($GF = \Delta R/R_0/\varepsilon$) [28, 29]. As the strain sensors are typically manufactured by combining flexible/stretchable supporting materials with electrically conductive active materials, their strain sensitivity is normally enhanced by exploring novel sensing materials such as low dimensional nanomaterials including metal nanowires [30], nanoparticles [31], carbon blacks [32], and carbon nanotubes [33]. Further, flexible/stretchable strain sensors based on thin film metal nanomaterials/elastic polymers are extensively explored strain sensors by virtue of their low cost and ease of fabrication. Lee et al. reported a metal nanoparticle/PDMS based strain sensor with a strain sensing range up to 20% through opening and closing of microcracks but it is inapplicable for full range human motion detection where strain levels can reach as high as 55% [34]. In another study, strain sensing range up to 10% have been achieved through conductive network of ionic liquids but they exhibit low sensitivity or gauge factors of 2.5 [35]. To achieve strain sensors with high sensitivity and a broad strain-sensing range simultaneously, AgNWs have been extensively employed as active sensor materials due to their unique electrical, mechanical and optical characteristics [36–38]. The high aspect ratio of silver nanowires makes the adjacent nanomaterials entangled to form an electrically conductive percolative network. When stretching strains are applied, the network breaks down and then reconstruct when the strain is reversed which results in measurable and recordable electrical resistance variation. Various investigations have been carried out on the flexible/stretchable resistive-type strain sensors based on silver nanowires combined with elastic polymers.

The inkjet printing method has been demonstrated to be an efficient technology for fabricating electronic devices [39–43]. When compared with traditional fabrication methods such as photolithography, stamping, vacuum deposition, electroless plating and stencil/screen printing, inkjet printing exhibit several advantages in high volume manufacturing and controlled patterning. The inkjet printing method has been widely used for the fabrication of various electronic devices such as sensors [44, 45], supercapacitors [46, 47], thin film transistors (TFTs) [48, 49], photodetectors [50], and optoelectronics [51, 52] owing to its capability to endow the devices with excellent mechanical, optical and electrical properties.

Herein, this research reports a highly sensitive, stretchable, and biocompatible strain sensor with remarkable durability for wearable sensing applications. Precise sensing and monitoring of human motion has been carried out owing to the embedded nanonetwork of silver nanowires (AgNWs) on the surface of ecoflex elastomer in straight line type and notched line type configurations. The fabrication process involves the inkjet printing of thin AgNW networks on poly(ethylene terephthalate) (PET) substrates, followed by their transfer onto the top surface of the Ecoflex film. In this work, epidermal-like ecoflex elastomer was chosen with low Young's modulus ($E = 125$ kPa) as a stretchable substrate for the fabrication of strain sensors to achieve a large dynamic strain sensing range, flexibility, durability, biocompatibility and attachability onto the human epidermis. The key novelty and contribution of this work is the chemistry for silver nanomaterial deposition with inkjet printing and the systematic testing of dynamic sensing performance of strain sensors under different conditions has been conducted. For example, the critical sensing properties of the wearable strain sensors have been evaluated such as stretchability or strain sensing range, sensitivity, linearity, hysteresis performance, and reproducibility. The straight line type and notched line type strain sensors exhibit a strain sensing range over 30%, a high gauge factor of 12.3 and 13.7, high linearity ($R^2 > 0.99$ and 0.98) over the strain sensing range, low hysteresis and long-term durability and stable repeatability for over 1000 stretch-release cycles. Finally, the wearable device was demonstrated for the detection and real-time

monitoring of facial expressions, bending process of the finger, wrist, elbow and knee joints for potential applications in human motion/health monitoring.

2 Experimental section

2.1 Materials

The Smooth-On Inc Ecoflex 00-30 (Part A (molecular weight = 28,000) and Part B (molecular weight = 37,000)) silicone elastomer and Skin Tite (Part A and Part B) were purchased from ONS Impex Traders Private Limited (Mumbai, India). Silver nitrate ($AgNO_3$), potassium bromide (KBr), potassium iodide (KI), sodium carbonate anhydrous, sodium sulphite anhydrous, and hydroquinone were supplied by S.D. Fine Chemicals (India). All the chemicals were of AR grade and used as purchased without further purification. The inkjet printer (1112) and HP 803 black ink cartridges were purchased from Hewlett Packard (HP, India).

2.2 Preparation of printing structure and electrically conductive pattern

A large piece of poly(ethylene terephthalate) (PET) was cut and secured onto a paper substrate by a double-side tape. The rectangular and notch shaped electrically conductive patterns of dimensions of 40 mm × 4 mm were achieved on PET substrate by inkjet printing alternative layers of potassium halide (KBr:KI:95:5 volume based) and silver nitrate ($AgNO_3$) followed by exposing the obtained silver halide film to a commercially available halogen lamp (Crompton Greaves, 500 W, 240 V, and luminous intensity of 9500 cd) for 10 min and treatment with a D-72 chemical developing agent for 10 min (Fig. 1a–c). The obtained AgNW thin film was then rinsed with DI water and dried in vacuum desiccators. The A and B parts of Ecoflex silicone elastomer were combined in a weight ratio of 1A:1B and mixed thoroughly and poured onto the AgNW/PET composite. The Ecoflex/AgNW/PET composite was then left to cure and dry for over 4 h at room temperature before removing the AgNW/Ecoflex composite from the PET substrate. Electrical wires and silver paste electrodes were applied to the two ends of the AgNW/Ecoflex composite to reduce to contact resistance. The AgNW/Ecoflex composite was then sealed using another slab of Ecoflex to obtain Ecoflex/AgNW/Ecoflex sandwich structured strain sensors (Fig. 1d).

Figures 2g, h, i and 3i, j, k shows the digital photographs of inkjet printed AgBrI thin film, inkjet printed AgNW conductive network, and Ecoflex/AgNW/Ecoflex sandwich structured nanocomposite based strain sensor with straight line type and notched line type configurations which clearly demonstrate the uniformity of the inkjet printed patterns of the fabricated strain sensors which is desirable for obtaining stable electrical resistance responses. In order to compare the strain sensing performance or strain sensitivity for the Ecoflex based wearable strain sensors, two types of devices (Straight line type and notched line type AgNW conductive network) were fabricated. A notch was created on the AgNW conductive network by changing the digital print pattern in MS PPT. The role of notching is to restrict the electron conduction pathway and effectively enhance the strain sensitivity of the electrically conductive film. With notching, the AgNW conductive network cannot effectively absorb the mechanical strains, which shows that notching of the electrically conductive film is favourable for obtaining improved resistance responses.

2.3 Fabrication of adhesive component

The A and B parts of the Skin Tite with a weight ratio of 1A:1B were mixed thoroughly and spread evenly and thinly onto the backside of Ecoflex/AgNW/Ecoflex sandwich structured strain sensors.

2.4 Characterization

The morphologies of the inkjet printed AgNW patterns were characterized using scanning electron microscopy (SEM, Zeiss-Ultra 55). Gold sputtering was carried out prior to SEM observation. The devices were fixed in between the two grippers of tensile testing machine (Mecmesin, UK) which comprised of a static unit and an actuating part and uniform stretch-release cycles were applied at different applied strains and stretching frequencies. Real-time resistance variations of the Ecoflex/AgNW/Ecoflex sandwich structured strain sensors were measured with a Keithley 2450 digital sourcemeter at room temperature. Detection of various human motions was carried out by attaching the wearable strain

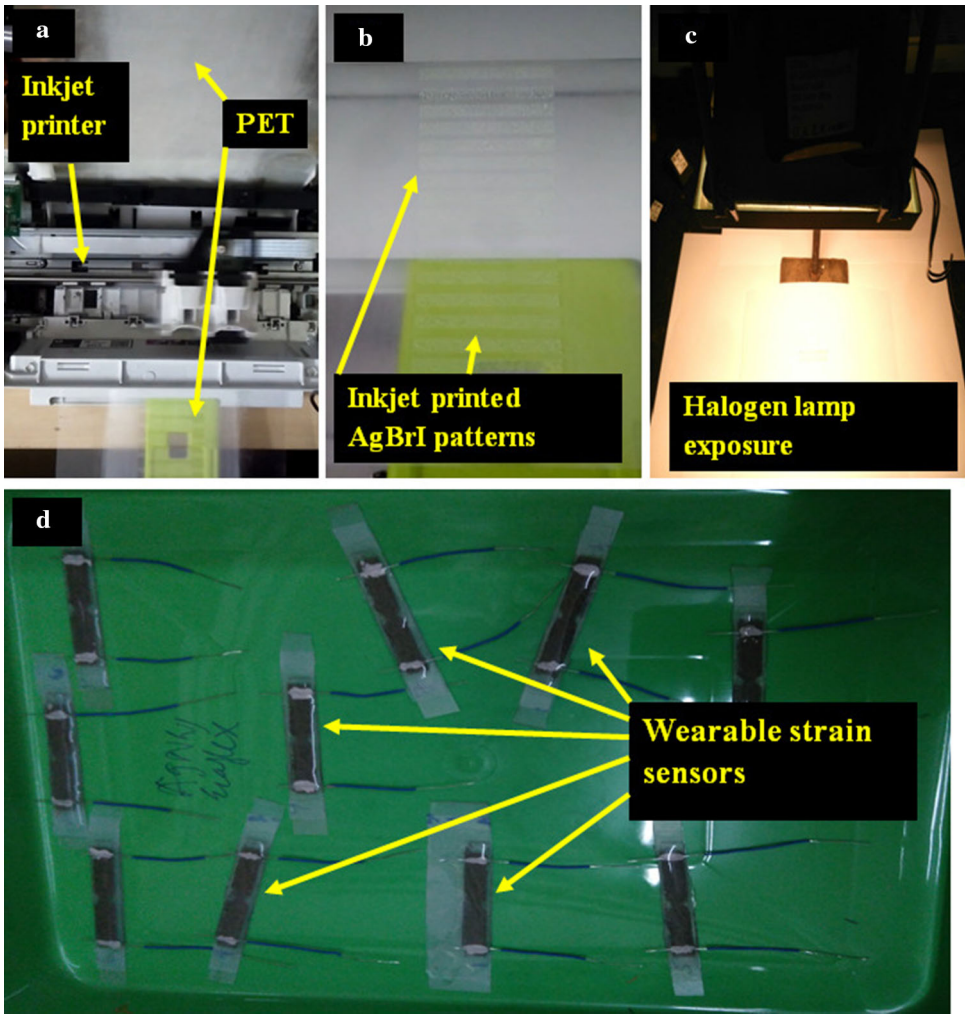

Fig. 1 A representative diagram of the steps followed for inkjet printing of silver nanostructures to fabricate printed strain sensors **a** Inkjet printer for printing KBr/KI and $AgNO_3$ functional materials for achieving AgBrI thin films on PET substrates. **b** Inkjet printed AgBrI patterns on PET substrates. **c** The process of photolytic reduction of AgBrI films using a commercial halogen lamp. **d** Digital photographs of inkjet printed skin-like stretchable, and wearable strain sensors

sensors onto the respective joints using Skin-Tite (Smooth-On).

3 Results and discussion

3.1 Fabrication of the AgNWs/Ecoflex composite based highly stretchable strain sensor

The fabrication procedure of the straight line type and notched line type AgNW/Ecoflex nanocomposite based strain sensor is schematically illustrated in Figs. 2 and 3, and the detailed fabrication procedure is given in the experimental section. In the first step, the AgNW conductive network was obtained on the poly(ethylene terephthalate) substrate by a reactive inkjet printing process. The chemical equations for the transformation of silver halide thin film into silver nanomaterials are provided in Eqs. 1, 2, and 3.

$$\text{Photolytic reduction}: \ \mathrm{AgX} + \mathrm{h}v \rightarrow e^- + h^+ \quad (1)$$

$$\text{Nucleation}: \ kink + pe^- + p\mathrm{Ag}^+ \rightarrow kink\mathrm{Ag}_p \quad (2)$$

$$\text{Growth}: \ q\mathrm{Ag}^+ + \text{Chemical Developer} \xrightarrow{kink\mathrm{Ag}_p} q\mathrm{Ag} + \text{Oxidized Chemical Developer} + m\mathrm{H}^+ \quad (3)$$

Next, the Ecoflex liquid (00–30) was transferred onto the surface of AgNW conductive network and cured at room temperature for 4 h to obtain the Ecoflex elastomer in the solid form. The obtained solid Ecoflex was then peeled off the AgNW conductive network to achieve AgNW/Ecoflex composite.

Scanning electron microscopy (SEM) analysis was conducted to characterize the morphology and

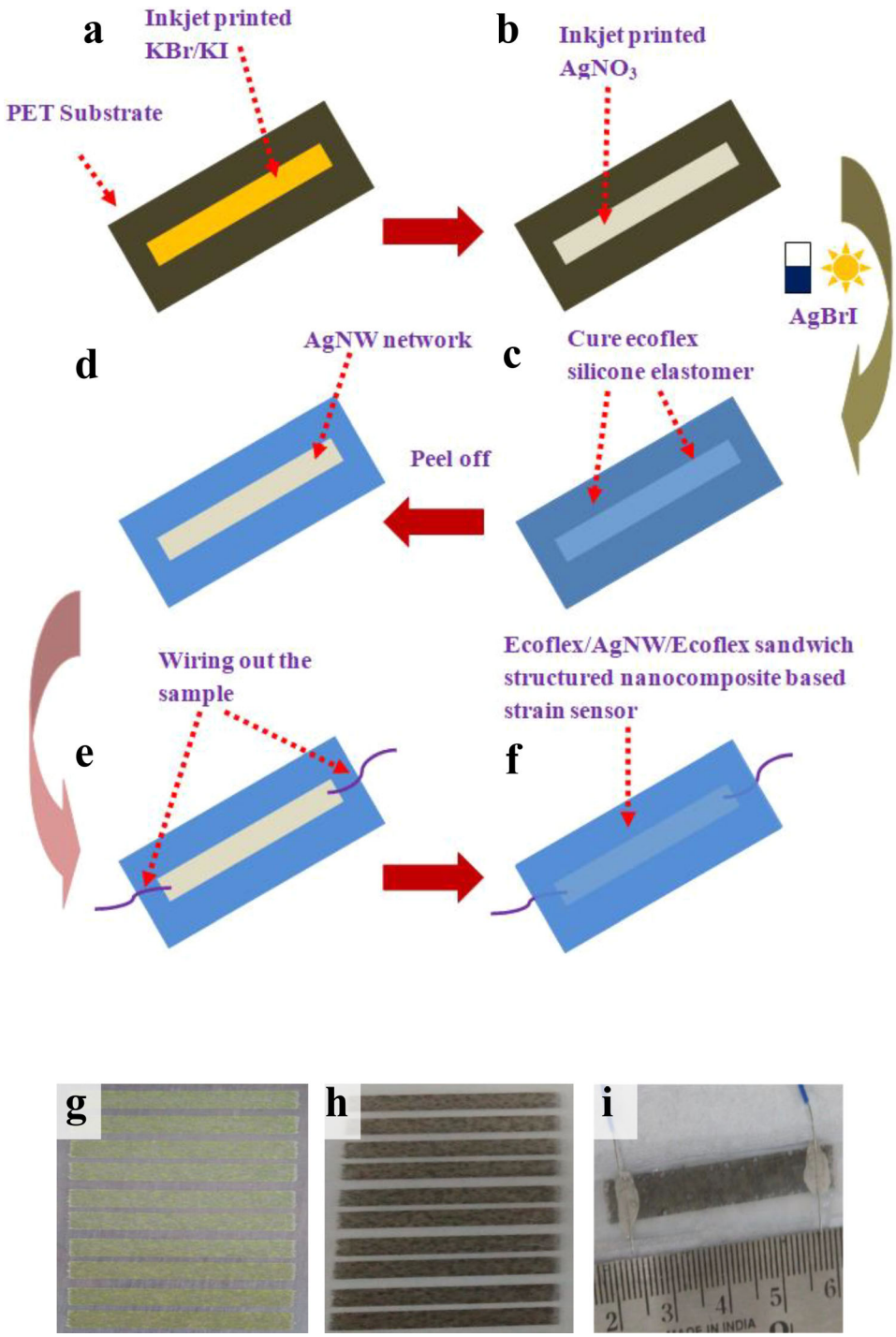

Fig. 2 Schematic diagram of the fabrication process of the straight line type strain sensor. **a** Inkjet print KBr/KI onto the PET substrate. **b** Inkjet print $AgNO_3$ onto the KBr/KI pattern. **c** Pour and impregnate the AgNW conductive network with uncured Ecoflex. **d** Peel off the Ecoflex substrate after the curing process. **e** Attach electrical wires with silver paste. **f** Encapsulate and seal the whole device with Ecoflex. **g** Photograph of the AgBrI thin film. **h** Photograph of the AgNW conductive network. **i** Photograph of the sandwich structured nanocomposite-based strain sensor

microstructure of the as-prepared AgNWs/Ecoflex nanocomposites at different magnifications. As shown in Fig. 4a, b, the sample is composed of both nanowires and nanoparticles. After the inkjet printing (Fig. 1a, b), photo-exposure (Fig. 1c), and development procedure of AgBrI films, an electrically conductive network comprising of nanowires was successfully achieved. The SEM images further indicate the existence of pores embedded in the AgNWs conductive network. While stretching the wearable device, the evolution of porous conductive network would occur and this would be beneficial for the enhancement of strain sensitivity.

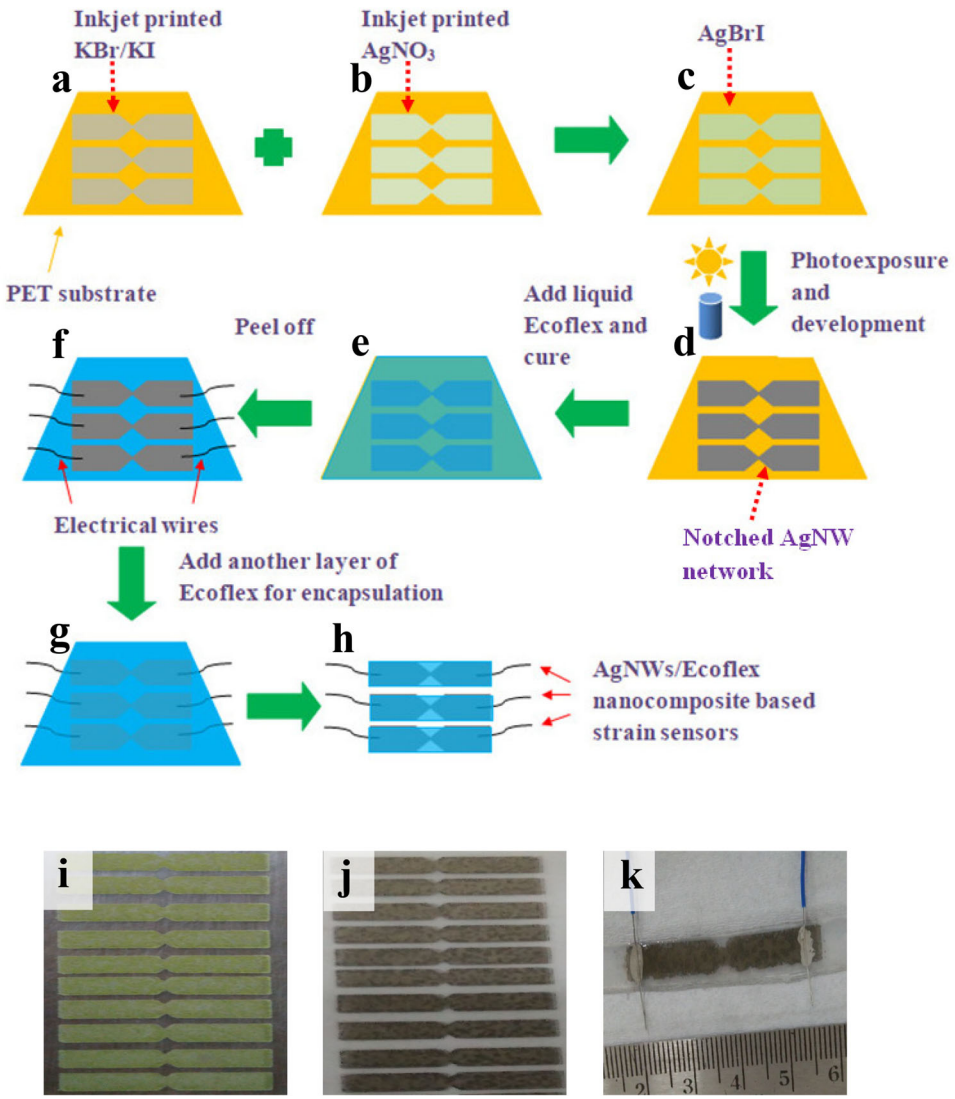

Fig. 3 Schematic diagram of the fabrication process of the notched line type strain sensor. **a** Inkjet print KBr/KI onto the PET substrate. **b** Inkjet print $AgNO_3$ onto the KBr/KI pattern. **c** Formation of AgBrI thin films. **d** Formation of AgNW conductive network. **e** Pour and impregnate the AgNW conductive network with uncured Ecoflex. **f** Peel off and attach electrical wires with silver paste. **g** Encapsulate and seal the whole device with Ecoflex. **h** Notched line type strain sensors. **i** Photograph of the AgBrI thin film. **j** Photograph of the AgNW conductive network. **k** Photograph of notched line type strain sensor

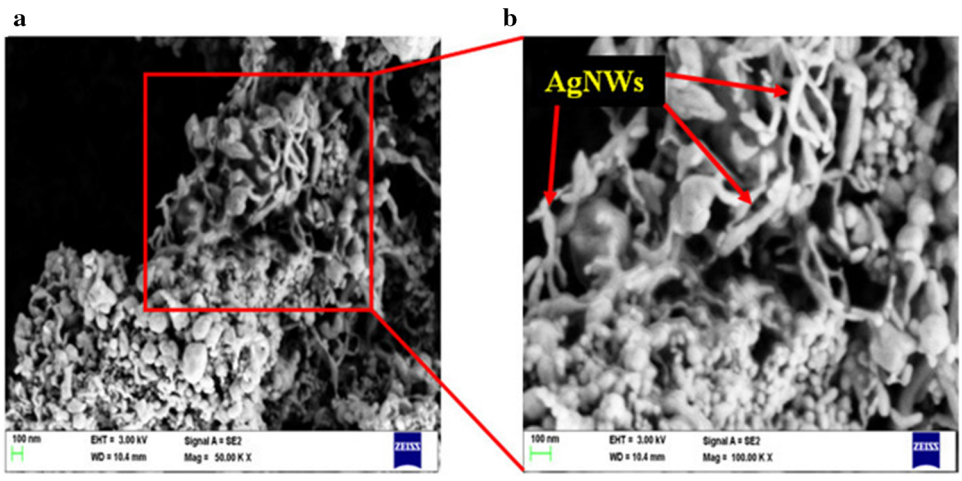

Fig. 4 **a** SEM images of straight line type AgNWs conductive network at a magnification of 50,000× . **b** SEM images of straight line type AgNWs conductive network at a magnification of 100,000×

3.2 Electromechanical performance of the Ecoflex/AgNW/Ecoflex sandwich structured nanocomposite based strain sensor

Figure 5a shows the relative resistance variations of straight line type and notched line type Ecoflex/AgNW/Ecoflex sandwich structured nanocomposite based strain sensors. The strain sensors based on the straight line type and notched line type configurations exhibited a strain sensing range over 30% strain. The electrically conductive film was prepared with reactive inkjet printing process using silver nitrate and potassium halide concentration of 1 M and 2 M, respectively, which are described in detail in the experimental section. It is clear that the relative resistance signal of straight line type strain sensor is much lower than that of notched line type device. The notching of the electrically conductive film results in the reduction in the surface area, overlapped area and the interfacial bonding between the AgNW conductive network and Ecoflex elastomer. These structural changes significantly decrease the electron conduction pathway and results in the enhancement in electrical resistance response. Figure 5b shows the $\Delta R/R_0$ values at small-scale mechanical strains.

The electromechanical characteristics of the AgNW/Ecoflex nanocomposite strain sensors were evaluated by gripping the electronic devices on the tensile testing machine to investigate their sensing performance under various stretching-releasing dynamic strains. The strain rates and the applied strain levels were effectively controlled, and the electrical resistance values were recorded using a digital sourcemeter connected to the strain sensor (Keithley 2450). The applied dynamic tensile strain varied from 5 to 30%, while the strain rates were 50 mm/min, 100 mm/min, 150 mm/min, and 200 mm/min for various studies. Durability

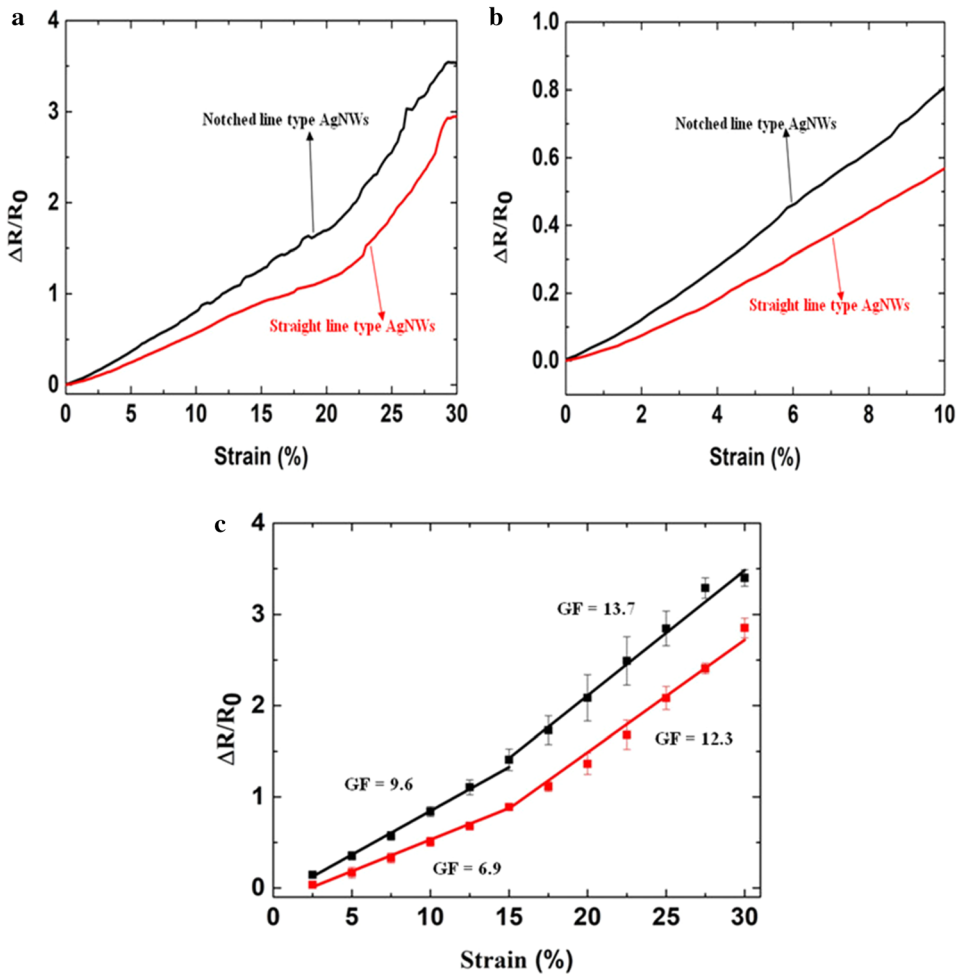

Fig. 5 **a** Relative resistance variations of the straight line type and notched line type Ecoflex/AgNW/Ecoflex sandwich structured nanocomposite based strain sensors while stretching. **b** Relative resistance variations of the straight line type and notched line type Ecoflex/AgNW/Ecoflex sandwich structured nanocomposite based strain sensors under small-scale mechanical strain. **c** Relative resistance variations of the strain sensors based on straight line type and notched line type Ecoflex/AgNWs/Ecoflex sandwich structured nanocomposites from 2.5% to 30% strain. Extraction of the gauge factors by linearly fitting the plot of the relative resistance variation as a function of the applied strain

investigations were carried out over 1000 stretching-releasing cycles under 10% tensile strain on the same universal testing machine. All experiments were conducted at room temperature. Figure 5c shows relative resistance variations ($\Delta R/R_0$) of straight line type and notched line type Ecoflex/AgNW/Ecoflex sandwich structured nanocomposite-based strain sensors. The strain sensitivity was evaluated by the gauge factor (GF), which is defined as $(\Delta R/R_0)/\varepsilon$, where $(\Delta R/R_0)$ is the relative resistance variation and ε is the mechanical strain. The gauge factor values of the straight line type and notched line type Ecoflex/AgNW/Ecoflex nanocomposite based strain sensor are 6.9 and 9.6 (strain range: 0–15%), and 12.3 and 13.7 (strain range: 15–30%), respectively, indicating that the notching of the electrically conductive film has a significant influence on the strain sensing performance of the wearable strain sensor. The notched line type Ecoflex/AgNW/Ecoflex sandwich structured nanocomposite based strain sensor exhibit higher values of gauge factors because the electron conduction pathway and overlapped area between Ecoflex and AgNW conductive network has been significantly reduced. The higher gauge factor values demonstrate that the device could have better strain sensitivity. In this research, the largest gauge factor value of 13.7 is obtained in the strain range of 15–30% with the notched line type Ecoflex/AgNW/Ecoflex sandwich structured nanocomposite based strain sensor.

Figure 6 shows the relative resistance variations of an Ecoflex/AgNW/Ecoflex sandwich structured nanocomposite based strain sensor under cyclic loading–unloading at different external strains with the same applied strain rate. As the external strain is increased, the change is electrical resistance value increases but the initial electrical resistance value can be completely recovered after each loading/unloading cycle.

Fast responsiveness to external mechanical stimuli is another criterion for consideration for practical wearable sensors and devices. The response time of the straight line type and notched line type Ecoflex/AgNW/Ecoflex sandwich structured nanocomposite based strain sensor was also investigated and the corresponding results are shown in Fig. 7. The experimental results reveal that the response time of the straight line type and notched line type Ecoflex/AgNW/Ecoflex sandwich structured nanocomposite based strain sensors could be lower than 600 ms and 500 ms, respectively which demonstrate the fast responsiveness of the fabricated strain sensors.

Figure 8 shows the hysteresis curves of the straight line type and notched line type Ecoflex/AgNW/Ecoflex sandwich structured nanocomposite based strain sensor. The hysteresis is relatively small when external strain is 5% for a loading/unloading cycle. For larger external strains (ε = 10%, 20%, and 30%), the hysteresis error is slightly larger but the electrical resistance can still be regained to its original resistance value after a loading/unloading cycle which

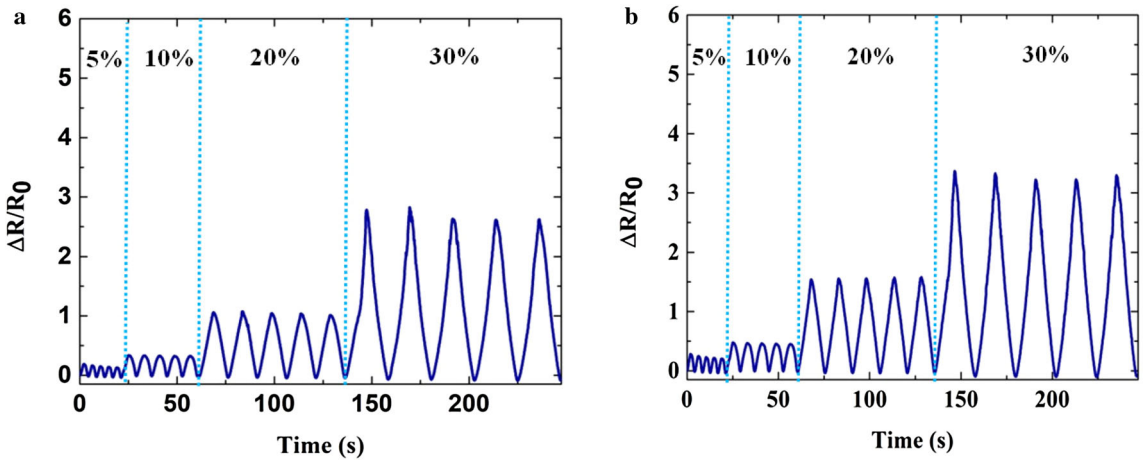

Fig. 6 Relative variations in strain sensor resistance under various dynamic strains: **a** Relative resistance variation under different stretching strains for straight line type Ecoflex/AgNW/Ecoflex sandwich structured nanocomposite based strain sensor. **b** Relative resistance variation under different stretching strains for notched line type Ecoflex/AgNW/Ecoflex sandwich structured nanocomposite based strain sensor

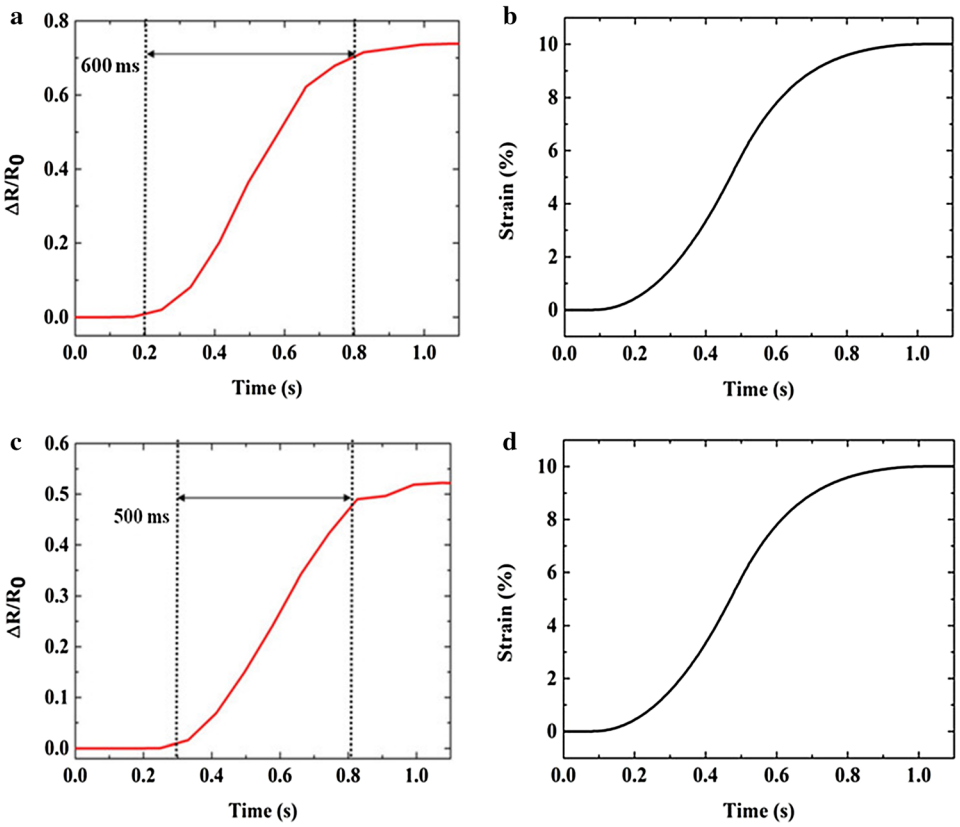

Fig. 7 Relative variations in strain sensor resistance under various dynamic strains: **a** Instant strain responsiveness to small-scale stretching, i.e., the relative resistance of the straight line type strain sensor for 0–10% strain. **b** The applied tensile strain profile. **c** Instant strain responsiveness to small-scale stretching, i.e., the relative resistance of the notched line type strain sensor for 0–10% strain. **d** The applied tensile strain profile

demonstrates the remarkable strain sensing performance of the Ecoflex/AgNW/Ecoflex sandwich structured nanocomposite based strain sensors.

The peculiar hysteretic characteristics of the AgNW/Ecoflex nanocomposite is observed where the sensor deforms linearly as the applied strain increases and the unloading curve finally regains its original value with negligible plastic impairment, indicating that the strain sensor can withstand extensive mechanical deformations. The loop observed in the electrical response denotes the energy dissipation during the dynamic stretch-release cycles. The ability of energy dissipation results from the disentanglement of elastomer chains and sensor networks as well as rupturing of cross-linking regions [53, 54]. Hysteretic characteristics majorly occur on account of the viscoelasticity of elastomeric matrix and as a result of interfacial sliding between the sensor networks and elastic polymers [55–57], as well as thermal conductivity of the composite materials [58]. The interaction between active materials and elastomer chains occur due to the van der Waals forces and the interfacial slippage happen during the dynamic stretch-release cycles leading to the dissipation of frictional energy. [59].

To investigate the strain-sensing performance of AgNWs/Ecoflex nanocomposite strain sensors at different tensile strain rates, the devices were subjected to 10% strain in stretch-release cycles as shown in Fig. 9a, b. When the applied strain rate varies from 50 mm/min to 200 mm/min, the shape of the relative resistance signal conforms well, that is, the performance characteristics is not deteriorated with the increase in tensile strain rate, indicating that the output electrical signal is frequency independent. Figure 10a, b compares the performance characteristics for different applied strain rates. The data plots demonstrate negligible hysteretic characteristics for each strain rate and represent independency of electrical signal output to the applied strain rates in the range of $d\varepsilon/dt$ = 50–200 mm/min.

For practical and real-life applications, a wearable strain sensor is required to maintain its strain sensing performance without significant fatigue failure. In order to investigate the stability, reliability and long term durability of the wearable strain sensor, 1000 cycles of repeated loading/unloading cycles with a

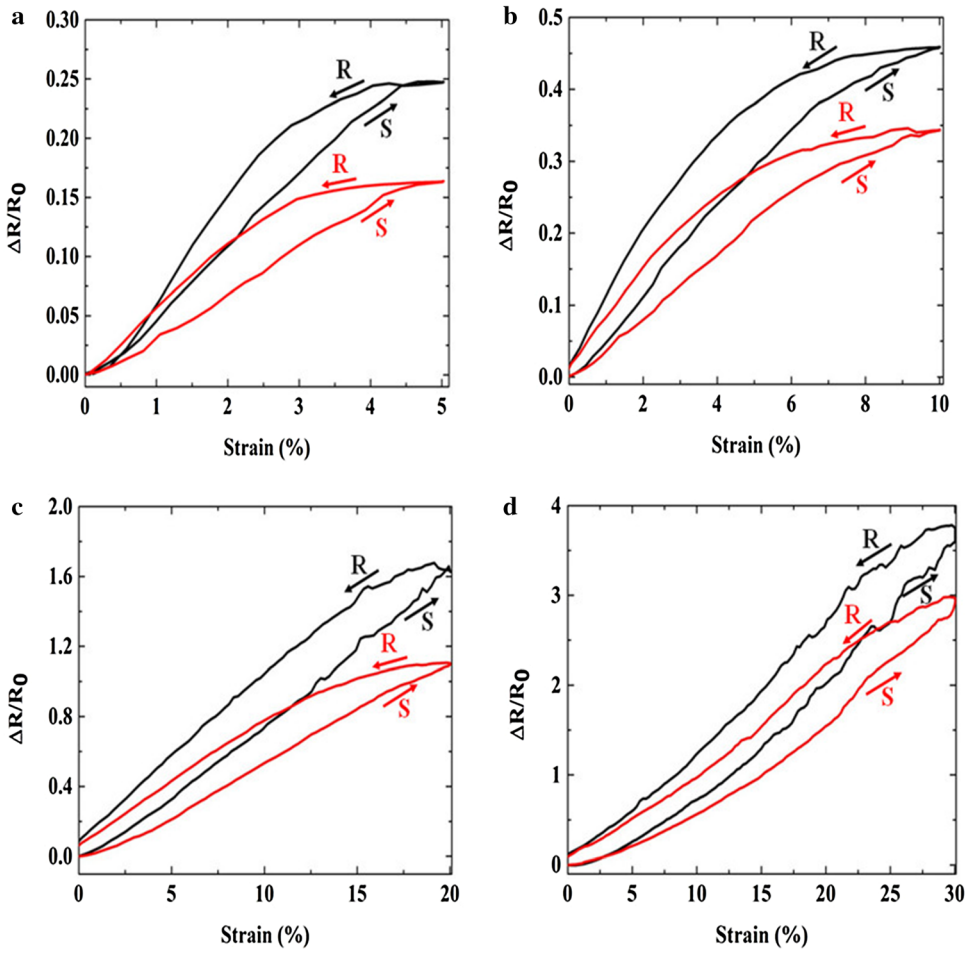

Fig. 8 Relative variations in the strain sensor resistances based on straight (red) and notched line type (black) Ecoflex/AgNWs/Ecoflex sandwich structured nanocomposite based strain sensor under a stretching and releasing cycle. **a** strain from 0% to 5% to 0%. **b** strain from 0% to 10% to 0%. **c** strain from 0% to 20% to 0%. **d** strain from 0% to 30% to 0%. In the plots, S denotes stretching and R denotes releasing

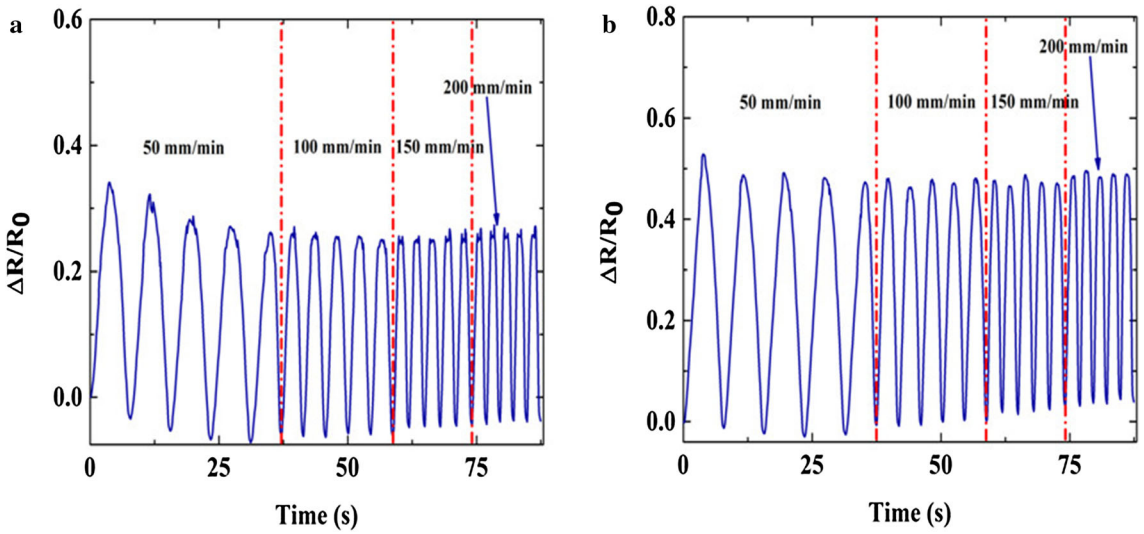

Fig. 9 The relative resistance variation of AgNWs/Ecoflex nanocomposite based strain sensor under dynamic strains. **a** Relative resistance variation of straight line type AgNWs/Ecoflex device under different strain rates. **b** Relative resistance variation of notched line type AgNWs/Ecoflex device under different strain rates

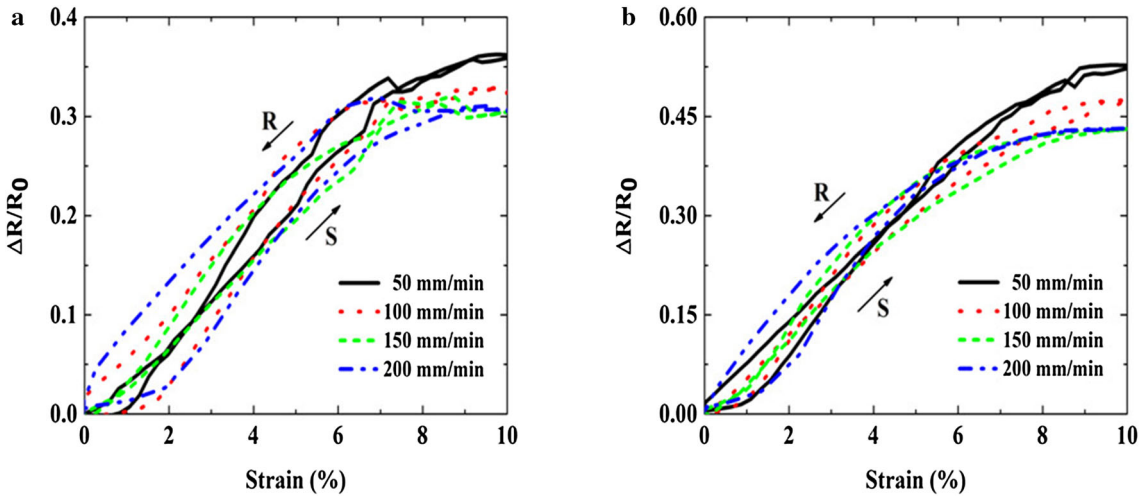

Fig. 10 The relative resistance variation of AgNWs/Ecoflex strain sensor under small-scale dynamic stimuli. **a** Relative resistance variation of the straight line type AgNWs/Ecoflex strain sensor under a stretching and releasing cycle for different stretching strain rates. In the plot, S denotes stretching and R denotes releasing. **b** Relative resistance variation in the notched line type AgNWs/Ecoflex strain sensor under a stretching and releasing cycle for different stretching strain rates. In the plot, S denotes stretching and R denotes releasing

large strain of ε = 10% were applied to the straight line type and notched line type Ecoflex/AgNW/Ecoflex sandwich structured nanocomposite based strain sensor at a stretching frequency of 0.25 Hz. The corresponding results are shown in Figs. 11 and 12. The wearable strain sensor displays remarkable stability with low drift during 1000 cycles of loading/unloading without failure due to fatigue. For practical applications, the first 50 stretch-release cycles can be considered as a device "aging" process. From these investigations, we could observe that the sandwich structured strain sensors exhibit superior mechanical durability and stability for repeated stretching and releasing external strains.

In this research, it is worth to mention that the Ecoflex/AgNW/Ecoflex sandwich structured nanocomposite based strain sensor exhibit high sensitivity or gauge factor, a broad strain sensing range or stretchability, low hysteresis, fast responsiveness and prominent long-term durability.

In addition to stretching strains, the relative resistance variation of wearable strain sensors during the application of bending strains was also carried out. For the cyclic bending test, the stepper was propelled on one end of the strain sensor with the other end gripped and secured firmly. The bending angle (θ) was defined as the external angle of the both ends. The relative resistance variation enhanced

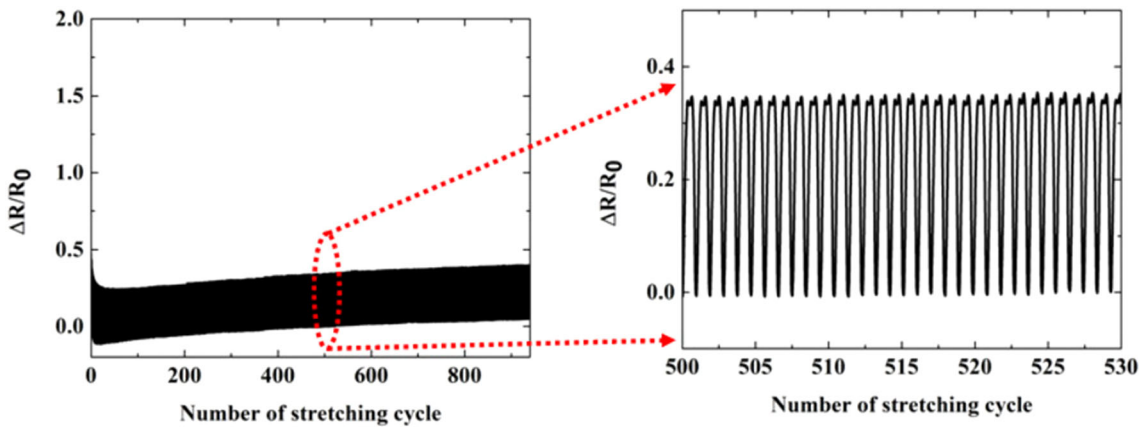

Fig. 11 Stability and durability test of the straight line type Ecoflex/AgNW/Ecoflex sandwich structured nanocomposite based strain sensor under 10% strain for 1000 cycles

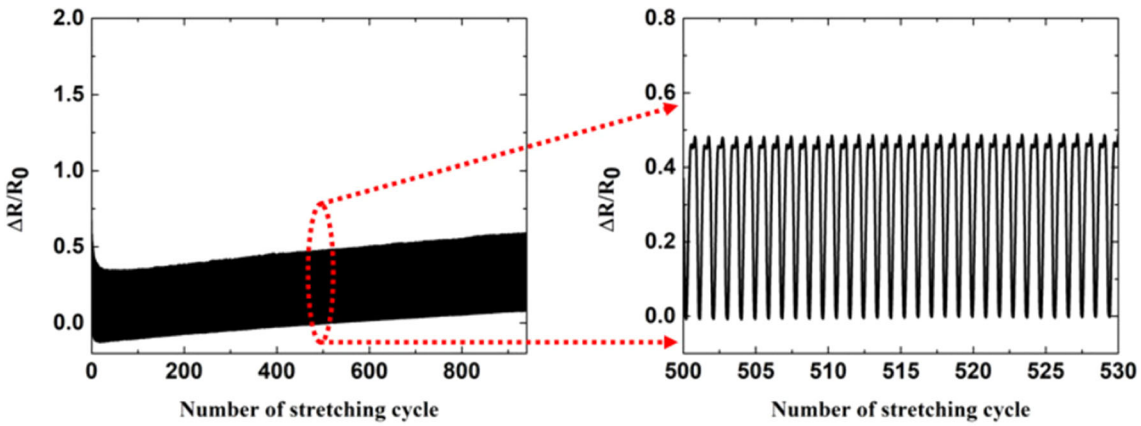

Fig. 12 Stability and durability test of the notched line type Ecoflex/AgNW/Ecoflex sandwich structured nanocomposite based strain sensor under 10% strain for 1000 cycles

prominently with compression bending. For instance, the relative resistance variation is 0.072 ± 0.011 for compression bending under the bending angle of 110° (Fig. 13a). The compression bending disconnects the adjacent nanomaterials significantly, resulting in an enhanced electrical resistance. The wearable strain sensor exhibits a reversible electrical response for bending deformations (Fig. 13b–d).

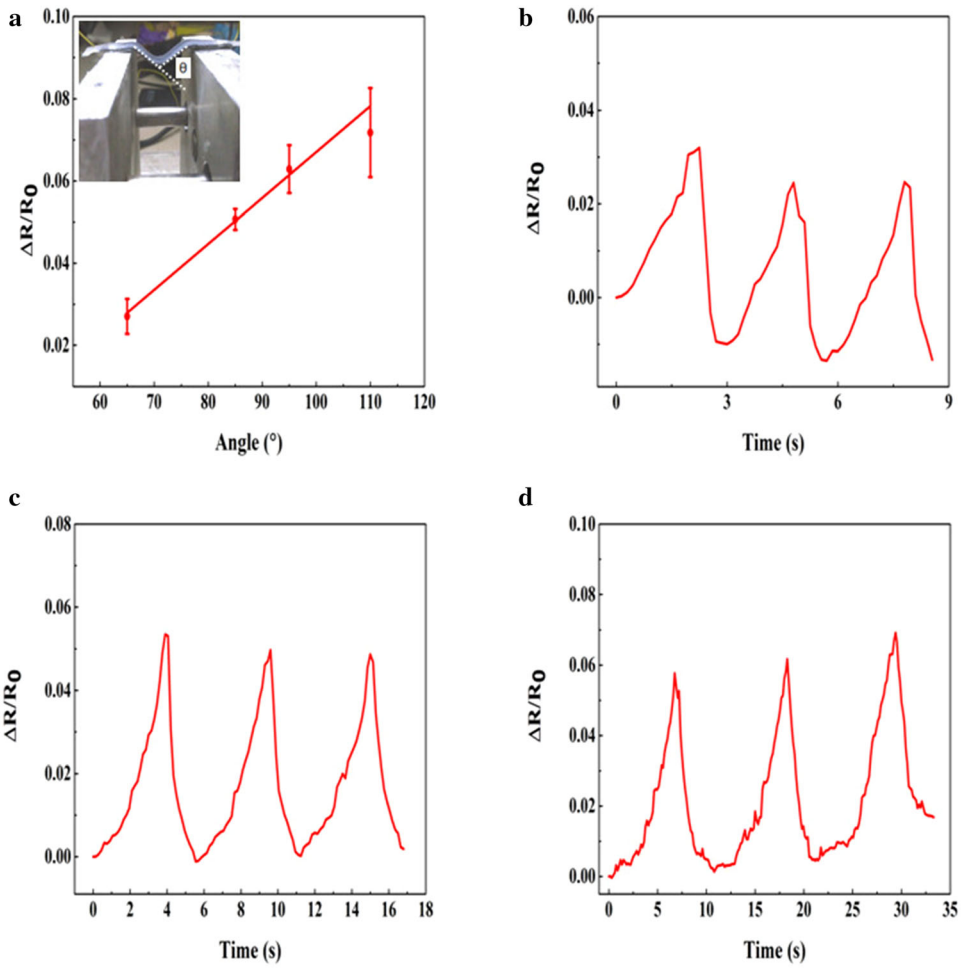

Fig. 13 **a** Relative resistance variation to bending deformation, compression (inward bending) of the strain sensor under bending angle of 65°, 85°, 95°, and 110°. (**b-d**) Relative resistance variations of the strain sensor during cyclic compression bending tests under bending angle of 65°, 85°, and 95°

3.3 Working mechanisms

Figure 14 shows the field emission scanning electron microscopy (FESEM) images of microstructures of the Ecoflex after embedding with AgNW conductive network and the surface morphologies of the AgNW conductive network. The AgNW particles are agglomerated and form a cluster on the Ecoflex surface with many pores in between. The surface of AgNW/Ecoflex exhibit many wrinkles which significantly enhance the specific surface areas and results in accommodating more AgNW particles onto the surface. The formation of wrinkle structure could be attributed to the shrinkage and stretching of Ecoflex during the peeling off stage from the poly(ethylene terephthalate) substrate. Moreover, due to the wrinkles, the thickness of the electrically conductive layer typically increases which results in lower original resistance of AgNW/Ecoflex nanocomposites.

The working mechanism of the Ecoflex/AgNW/Ecoflex sandwich structured strain sensor is based on the formation of percolating conductive network and mechanical deformation induced disconnection of adjacent AgNW particles, reduction in overlapped area and variations in the tunneling resistance of adjacent AgNW particles. As shown in Fig. 14a, at 0% strain, the surface of Ecoflex elastomer is embedded by many closely spaced AgNW particles in cluster form. Due to this, a good percolating and conductive network is obtained which results in high conductivity or low value of electrical resistance. When mechanical deformations are gradually applied (Fig. 14b), this conductive network is gradually deformed and elongation of porous structure occurs and finally results in a broken conductive network. This results in increment of spacing of the adjacent AgNW particles which in turn results in the enhancement of electrical resistance of nanocomposite based strain sensor. The junctions between two adjacent AgNW particles can be categorized into three classes depending on their distances, for instance, a complete contact, a tunneling conductive junction within a cut-off distance and a full disconnection of AgNW particles. The AgNW particles are said to be in complete contact when the shortest distance d between the centrelines of two adjacent AgNW particles is lesser or equal to the AgNW particle diameter D. When mechanically deformed, the electrons can cross through the elastomeric supporting material which triggers the tunneling of electrical currents in between the two noncontact AgNW particles and results in the formation of quantum conductive junction. This occurs when the distance d is larger than D but lower than the cut-off distance C. When the wearable strain sensor is deformed further, the distance among adjacent AgNW particles exceeds the cut-off distance C and in this case, the electrical connection is completely disconnected and electrons cannot cross through neighbouring or adjacent AgNW particles.

The strain sensitivity of the electrically conductive Ecoflex/AgNW/Ecoflex nanocomposite based strain sensor can be described as follows. Initially at an unstrained condition, a perfect electrically conductive percolative conductive network is present and the surface of elastomeric supporting material is covered by agglomerated clusters of AgNW particles. At this stage, the strain sensor exhibit low initial resistance and there is a complete contact between two adjacent AgNW particles. When the wearable strain sensor is

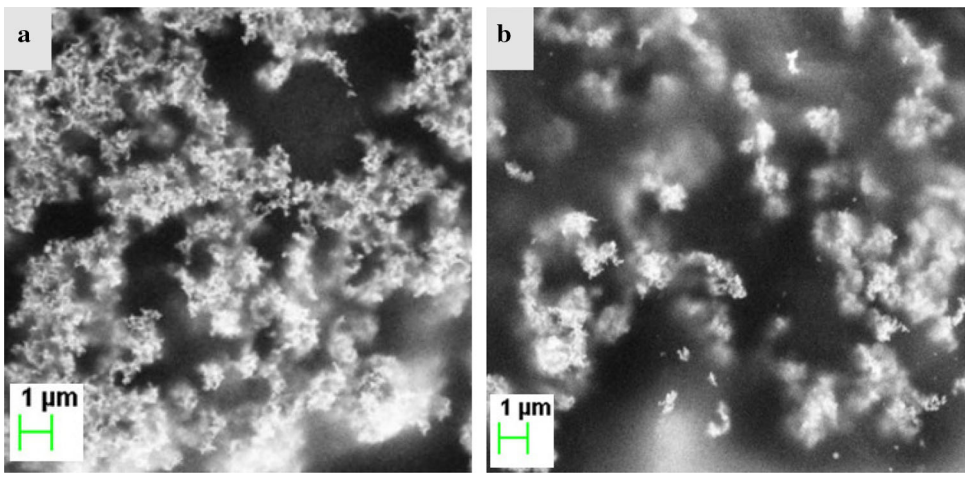

Fig. 14 SEM images of the AgNW/Ecoflex composite strain sensor under different strains: **a** 0%, and **b** 10%. The scale bar is 1 µm

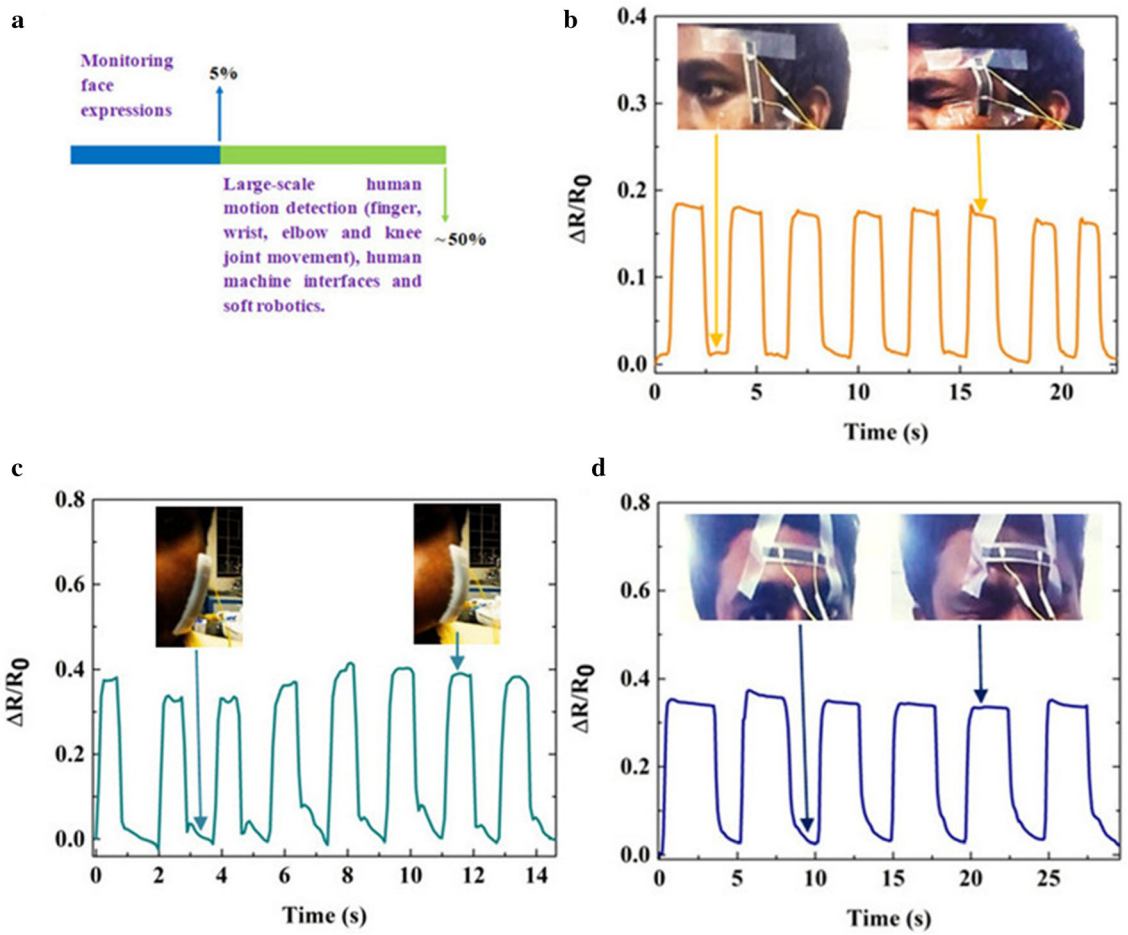

Fig. 15 **a** Schematic representation of the human activity and the corresponding strain scales involved. **b-d** Detection of small-scale human body deformations by the Ecoflex/AgNW/Ecoflex sandwich structured nanocomposite based strain sensor: **b** Eye blinking, **c** cheek movement, and **d** frown

stretched or mechanically deformed with a relatively minute strain, the closely spaced or packed AgNW particles are disconnected and nanogaps of several nanometers are formed which in turn results in the flow of tunneling currents. Within these minute strain limits, the junctions in between neighbouring AgNW particles exhibit a quantum conductive junction which results in the increment of electrical resistance of nanocomposite based strain sensor minutely as a function of external mechanical strain. When strained more, gradual disconnection of more AgNW particle occur which results in the alteration of junctions from complete contact mode to quantum tunneling junction. At this stage, the main conductive pathways for crossing of electrons are tunneling junctions which results in significant enhancement in electrical resistance. With further increase in external strain, more AgNW particles are further separated which results in the increment of distance beyond the cut-off distance between adjacent AgNW particles and the electrical pathway is fully disconnected and the electrical resistance increases to a very large value. The electrical resistance recovers its original value once the Ecoflex/AgNW/Ecoflex nanocomposite is reversed from the strained conditions and returns to its original state. This occurs due to the recovery of initial distance between adjacent AgNW particles after releasing the strain sensor from the strained state. Therefore, when the external strain is increased gradually, the junctions between neighbouring AgNW particles will be changed from a complete contact state to the formation of quantum tunneling junction followed by the full disconnection state. Correspondingly, the nanocomposite based strain sensor exhibit different strain sensitivity in

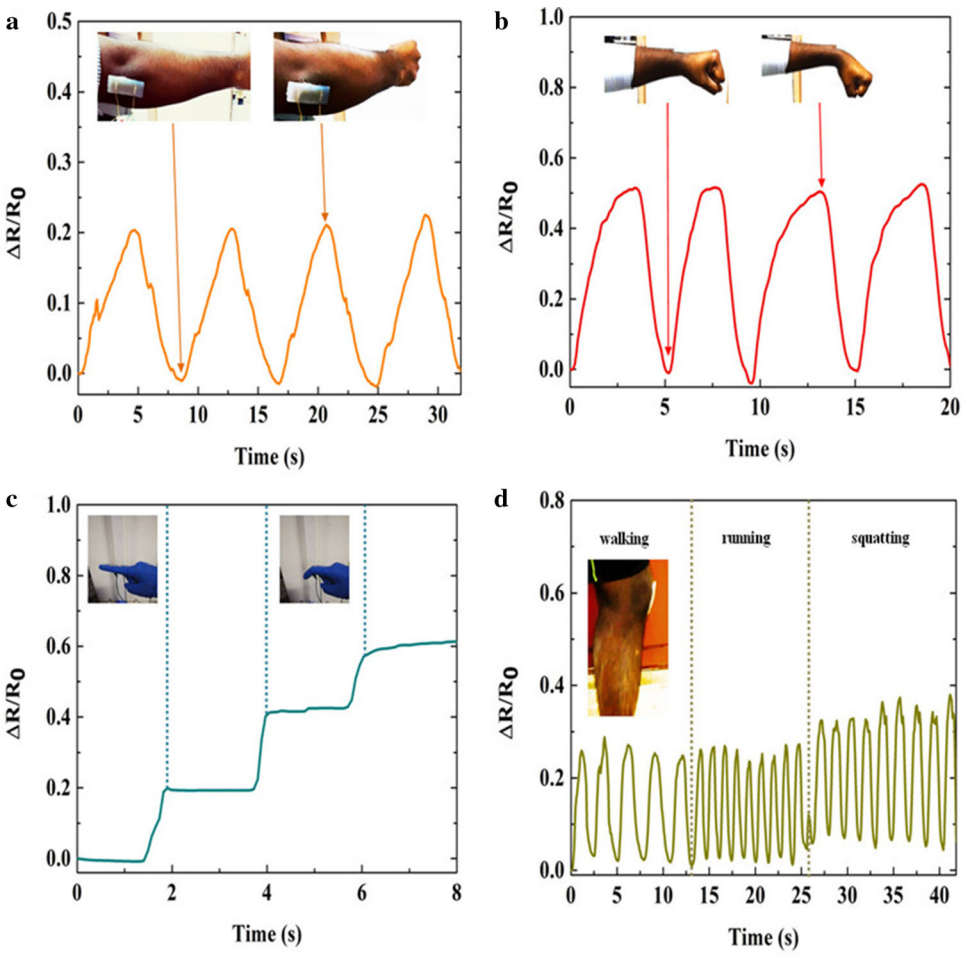

Fig. 16 Using the Ecoflex/AgNW/Ecoflex sandwich structured nanocomposite based strain sensor for human motion detection. **a** The relative variation in the strain sensor resistance mounted on elbow joint. **b** The relative variation in the strain sensor resistance mounted on wrist joint. **c** The relative variation in the strain sensor resistance mounted on finger joint to monitor bending process of a finger. **d** The relative variation in the strain sensor resistance for monitoring walking, running, and squatting of a knee joint

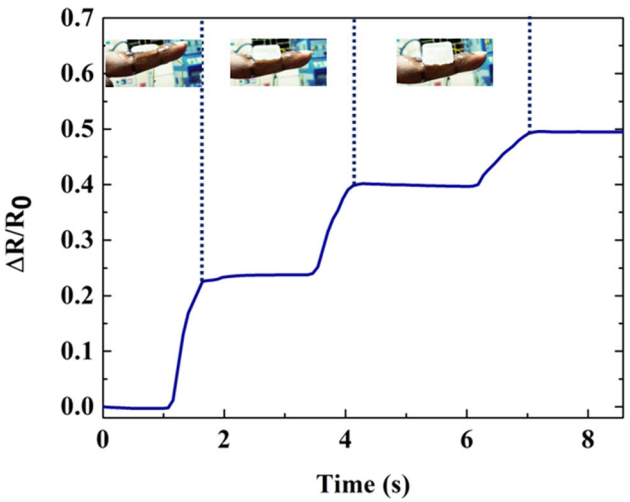

Fig. 17 Using the Ecoflex/AgNW/Ecoflex sandwich structured nanocomposite based strain sensor for human motion detection. The relative variation in the strain sensor resistance monitoring the closing process of the fingers

terms of gauge factors at different ranges of external strain.

3.4 Sensing demonstrations

The mechanical strains involved in human body deformations can be roughly categorised into two categories including small scale (<5%) and large scale mechanical deformations (~ 50%) as shown in Fig. 15a. In the further discussion, the Ecoflex/AgNW/Ecoflex sandwich structured nanocomposite based strain sensor is employed for multiscale sensing for real time monitoring of human body motions by attaching the sensor onto various human joints using Skin-Tite bioadhesive. The electrical response of the strain sensor was recorded every 80 ms using a digital sourcemeter (DSM). The wearable strain sensor was employed for monitoring the minute mechanical deformation of the human skin such as facial expressions. Apart from a substantial change in strain sensor resistance, the device should also

Table 1 Comparisons of the GFs against the maximum strain sensing range for previously reported strain sensors

Materials	Gauge factor (sensitivity)	Strain range (%)	Authors
CB/PDMS	5.5	10	Kong et al. [60]
Graphene/Glove	14	7.1	Bae et al. [61]
CNT/Polyurethane	6.42	0.8	Wang et al. [62]
CNT yarn	0.5	1	Zhao et al. [63]
CNT/Polyimide	6	1	Li et al. [64]
AgNP	2.8	0.1	Lee et al. [65]
PEDOT:PSS	0.53	0.3	Thompson et al. [66]
AgNP/Polyimide	6	1	Le et al. [67]
Ag flake/Polyimide	2.24	1.6	Park et al. [68]
AuNW/PDMS	7.38	25	Gong et al. [69]
AgNP/PDMS	2.05	20	Lee et al. [70]
AgNW/PDMS	20	35	Kim et al. [71]
AgNW/PEDOT:PSS	3.31	20	Eom et al. [72]
Pt/PUA/PDMS	11.5	5	Pang et al. [73]
Straight line type AgNW/Ecoflex	12.3	30	This Work
Notched line type AgNW/Ecoflex	13.7	30	This Work

exhibit mechanical deformation for a small scale strain. The elastomeric substrates such as Ecoflex elastic polymer typically exhibit low Young's modulus which results in sensitive reaction to applied strains. The internal muscle motions in the eyes, mouth and face express the human emotional state. For small scale sensing such as monitoring facial expressions, the device was mounted on a human canthus, mouth and forehead as shown in Fig. 15b, c, and d. For these motions, the wearable strain sensor can detect and monitor the small scale face motions by exhibiting an increase in electrical resistance. For monitoring different human body posture, the wearable strain sensor was integrated onto the finger joint as shown in Fig. 16c. As the finger bending angle increases, the resistance change increases in a stepwise fashion. The open and close finger positions can also be monitored by attaching the wearable strain sensor in between the two fingers (Fig. 17) using Skin-Tite (Smooth-On). Moreover, based on the amplitude and frequency of the motions, the strain sensor can also be attached onto the knee joint as shown in Fig. 16d for the detection and monitoring of human leg motion. Furthermore, in order to monitor the middle scale deformation, the wearable strain sensor was mounted on elbow (Fig. 16a), wrist (Fig. 16b) and knee joint (Fig. 16d) in order to record and monitor the bending process of each joint. During the cyclic bending process, the fabricated strain sensor exhibit favourable reproducibility and fast responsiveness. In this work, the noises due to external temperature change and type of surface were minimized by achieving a conformal contact with the human epidermis surface.

Finally, the strain sensing performance for previously reported strain sensors have been compared with the proposed strain sensors in Table 1.

4 Conclusions

In summary, this work demonstrated the construction of stretchable strain sensors with straight line type and notched line type AgNW conductive network incorporated within epidermis-like Ecoflex matrix. The AgNW conductive networks were achieved through a simple and scalable inkjet printing of silver nitrate and potassium halide solutions without the need for sintering or thermal processing. With regard to the sensing performance, in the strain range from 0% to 15%, the straight line type and notched line type stretchable strain sensors exhibit gauge factors of 6.9 and 9.6 under tensile strains and demonstrate a larger strain sensitivity with gauge factor values of 12.3 and 13.7 in the strain range from 15% to 30%. The inkjet printed stretchable strain sensors presented in this work demonstrate higher gauge factors than the strain sensors fabricated by different manufacturing processes and low

dimensional nanomaterials. The resistance variation, $\Delta R/R_0$ of the wearable strain sensors can be attributed to the intrinsic piezoresistive response, rearrangement of AgNW contacts and the variation of tunneling distance between the AgNWs caused due to the mechanical strain. The device demonstrate long term durability and reproducibility during multiple stretching cycles (∼ 1000 cycles) at 10% strain. The fabricated AgNW conductive network strain sensors are then applied to detect various human motions in real time. Moreover, the inkjet printing approach using silver nitrate and potassium halide precursor solutions can be effectively applied to manufacture stretchable AgNW strain sensors for emerging applications in biomedical engineering, electronic skin, touch sensing and beyond.

Declarations

Conflict of Interest The authors declare that they have no conflict of interest.

References

1. C. Luo, B. Tian, Yu. Qun Liu, W.W. Feng, One-step-printed, highly sensitive, textile-based, tunable performance strain sensors for human motion detection. Adv Mater Technol **5**(2), 1900925 (2020)
2. J. Ma, P. Wang, H. Chen, S. Bao, W. Chen, H. Lu, Highly sensitive and large-range strain sensor with a self-compensated two-order structure for human motion detection. ACS Appl. Mater. Interfaces **11**, 8527–8536 (2019). https://doi.org/10.1021/acsami.8b20902
3. W. Liu, Y. Huang, Y. Peng, M. Walczak, D. Wang, Q. Chen, Z. Liu, L. Li, Stable wearable strain sensors on textiles by direct laser writing of graphene. ACS Appl. Nano Mater. **3**, 283–293 (2020). https://doi.org/10.1021/acsanm.9b01937
4. Z.F. Liu, S. Fang, F.A. Moura, J.N. Ding, N. Jiang, J. Di, M. Zhang, X. Lepro, D.S. Galvao, C.S. Haines et al., Hierarchically buckled sheath-core fibers for superelastic electronics, sensors, and muscles. Science **349**, 400–404 (2015)
5. Yin Cheng, Ranran Wang, Kwok Hoe Chan, Lu. Xin, Jing Sun, Ghim Wei Ho, A biomimetic conductive tendril for ultrastretchable and integratable electronics, muscles, and sensors. ACS Nano **12**(4), 3898–3907 (2018)
6. Vu. Chicuong, J. Kim, Muscle activity monitoring with fabric stretch sensors. Fibers Polym **18**(10), 1931–1937 (2017)
7. T. Giorgino, P. Tormene, F. Lorussi, D.D. Rossi, S. Quaglini, Sensor evaluation for wearable strain gauges in neurological rehabilitation IEEE trans. Neural Syst. Rehabil. Eng. **17**, 409–415 (2009)
8. F. Porciuncula, A.V. Roto, D. Kumar, et al., Wearable movement sensors for rehabilitation: a focused review of technological and clinical advances [published correction appears in PM R. 2018 Dec;10(12):1437]. PM R. 10(9 Suppl 2), S220–S232. https://doi.org/10.1016/j.pmrj.2018.06.013 (2018)
9. S.-E. Park, Y.-J. Ho, M.H. Chun, J. Choi, Y. Moon, Measurement and analysis of gait pattern during stair walk for improvement of robotic locomotion rehabilitation system. Appl. Bionics Biomech. **2019**, 1495289 (2019)
10. Zewei Luo, Hu. Xiaotong, Xiyue Tian, Chen Luo, Xu. Hejun, Quanling Li, Qianhao Li, Jian Zhang, Fei Qiao, Wu. Xing, V. Borisenko, Junhao Chu, Structure-property relationships in graphene-based strain and pressure sensors for potential artificial intelligence applications. Sensors **19**(5), 1250 (2019)
11. S. Yao, P. Swetha, Y. Zhu, Nanomaterial-enabled wearable sensors for healthcare. Adv. Healthcare Mater. **7**(1), 1700889 (2018)
12. J. Guo, B. Zhou, R. Zong, L. Pan, X. Li, Yu. Xinguang, C. Yang, L. Kong, Q. Dai, Stretchable and highly sensitive optical strain sensors for human-activity monitoring and healthcare. ACS Appl. Mater. Interfaces. **11**(37), 33589–33598 (2019)
13. R. Rahimi, M. Ochoa, W. Yu, B. Ziaie, Highly stretchable and sensitive unidirectional strain sensor via laser carbonization. ACS Appl. Mater. Interfaces **7**, 4463–4470 (2015). https://doi.org/10.1021/am509087u
14. J. Huang, J. Zhou, Y. Luo, G. Yan, Yi. Liu, Y. Shen, Xu. Yong, H. Li, L. Yan, G. Zhang, Fu. Yongqing, H. Duan, Wrinkle-enabled highly stretchable strain sensors for wide-range health monitoring with a big data cloud platform. ACS Appl. Mater. Interfaces. **12**(38), 43009–43017 (2020)
15. X. Ye, Z. Yuan, H. Tai, W. Li, X. Du, Y. Jiang, A wearable and highly sensitive strain sensor based on a polyethylenimine–rGO layered nanocomposite thin film. J. Mater. Chem. C. **5**, 7746–7752 (2017). https://doi.org/10.1039/C7TC01872J
16. D.J. Cohen, D. Mitra, K. Peterson, M.M. Maharbiz, A highly elastic, capacitive strain gauge based on percolating nanotube networks. Nano Lett. **12**, 1821–1826 (2012). https://doi.org/10.1021/nl204052z
17. J.T. Muth, D.M. Vogt, R.L. Truby, Y. Mengüç, D.B. Kolesky, R.J. Wood, J.A. Lewis, Embedded 3D printing of strain sensors within highly stretchable elastomers. Adv. Mater. **26**, 6307–6312 (2014). https://doi.org/10.1002/adma.201400334
18. S. Liu, L. Li, Ultrastretchable and self-healing double-network hydrogel for 3D printing and strain sensor. ACS Appl.

Mater. Interfaces **9**, 26429–26437 (2017). https://doi.org/10.1021/acsami.7b07445
19. D. Zhang, Y. Tang, Y. Zhang, F. Yang, Y. Liu, X. Wang, J. Yang, X. Gong, J. Zheng, Highly stretchable, self-adhesive, biocompatible, conductive hydrogels as fully polymeric strain sensors. J Mater Chem A **8**(39), 20474–20485 (2020)
20. J. Lin, X. Cai, Z. Liu, N. Liu, M. Xie, BingPu Zhou, H. Wang, Z. Guo, Anti-liquid-interfering and bacterially antiadhesive strategy for highly stretchable and ultrasensitive strain sensors based on Cassie-Baxter Wetting State. Adv. Func. Mater. **30**(23), 2000398 (2020)
21. H. Zhang, N. Liu, Y. Shi, W. Liu, Y. Yue, S. Wang, Y. Ma, Li. Wen, L. Li, F. Long, Z. Zou, Y. Gao, Piezoresistive sensor with high elasticity based on 3D hybrid network of Sponge@CNTs@Ag NPs. ACS Appl. Mater. Interfaces. **8**(34), 22374–22381 (2016)
22. P. Feng, Y. Yuan, M. Zhong, J. Shao, X. Liu, Xu. Jie, J. Zhang, K. Li, W. Zhao, Integrated resistive-capacitive strain sensors based on polymer-nanoparticle composites. ACS Appl Nano Mater **3**(5), 4357–4366 (2020)
23. Z. Zhang, Q. Liao, X. Zhang, G. Zhang, P. Li, S. Lu, S. Liu, Y. Zhang, Nanoscale **7**, 1796–1801 (2015)
24. X. Liao, Z. Zhang, Z. Kang, F. Gao, Q. Liao, Y. Zhang, Mater. Horiz. **4**, 502 (2017)
25. J. Chen, J. Zheng, Q. Gao, J. Zhang, J. Zhang, O.M. Omisore, L. Wang, H. Li, Polydimethylsiloxane (PDMS)-based flexible resistive strain sensors for wearable applications. Appl. Sci. **8**, 345 (2018)
26. J. Chen, Q. Yu, X. Cui, M. Dong, J. Zhang, C. Wang, J. Fan, Y. Zhu, Z. Guo, J. Mater. Chem. C **7**, 11710–11730 (2019)
27. S. Wang, P. Xiao, Y. Liang, J. Zhang, Y. Huang, S. Wu, S.-W. Kuo, T. Chen, J. Mater. Chem. C **6**, 5140–5147 (2018)
28. Z. Zeng, Y. Yu, Y. Song, N. Tang, L. Ye, J. Zang, Precise engineering of conductive pathway by frictional direct-writing for ultrasensitive flexible strain sensors. ACS Appl. Mater. Interfaces **9**, 41078–41086 (2017). https://doi.org/10.1021/acsami.7b14501
29. T. Nguyen, M. Chu, R. Tu, M. Khine, The effect of encapsulation on crack-based wrinkled thin film soft strain sensors. Materials **14**, 364 (2021). https://doi.org/10.3390/ma14020364
30. Lim Wei Yap, Shu Gong, Yue Tang, Yonggang Zhu, Wenlong Cheng, Soft piezoresistive pressure sensing matrix from copper nanowires composite aerogel. Sci. Bull. **61**(20), 1624–1630 (2016)
31. G.-Y. Lee, M.-S. Kim, S.-H. Min, H.-S. Kim, H.-J. Kim, R. Keller, J.-B. Ihn, S.-H. Ahn, Highly sensitive solvent-free silver nanoparticle strain sensors with tunable sensitivity created using an aerodynamically focused nanoparticle printer. ACS Appl. Mater. Interfaces. **11**(29), 26421–26432 (2019)
32. H.B. Liu, H. Jiang, F. Du, D.P. Zhang, Z.J. Li, H.W. Zhou, Flexible and degradable paper-based strain sensor with low cost. ACS Sustain Chem. Eng. **5**, 10538–10543 (2017). https://doi.org/10.1021/acssuschemeng.7b02540
33. L. Cai, L. Song, P. Luan, Q. Zhang, N. Zhang, Q. Gao, D. Zhao, X. Zhang, M. Tu, F. Yang, W. Zhou, Q. Fan, J. Luo, W. Zhou, P.M. Ajayan, S. Xie, Super-stretchable transparent carbon nanotube-based capacitive strain sensors for human motion detection. Sci. Rep. **3**, 3048 (2013)
34. J. Lee, S. Kim, J. Lee, D. Yang, B.C. Park, S. Ryu, I. Park, Nanoscale **6**, 11932 (2014)
35. G. Keulemans, P. Pelgrims, M. Bakula, F. Ceyssens, R. Puers, An ionic liquid based strain sensor for large displacements. Procedia Eng. **87**, 1123–1126 (2014). https://doi.org/10.1016/j.proeng.2014.11.362
36. G.-J. Zhu, P.-G. Ren, H. Guo, Y.-L. Jin, D.-X. Yan, Z.-M. Li, Highly sensitive and stretchable polyurethane fiber strain sensors with embedded silver nanowires. ACS Appl. Mater. Interfaces. **11**(26), 23649–23658 (2019)
37. S. Yao, Y. Zhu, Wearable multifunctional sensors using printed stretchable conductors made of silver nanowires. Nanoscale **6**, 2345–2352 (2014). https://doi.org/10.1039/c3nr05496a
38. Yi Xi. Song, Xu. Wei Min, Min Zhi Rong, Ming Qiu Zhang, A sunlight self-healable transparent strain sensor with high sensitivity and durability based on a silver nanowire/polyurethane composite film. J Mater Chem A. **7**(5), 2315–2325 (2019)
39. D.J. Finn, M. Lotya, J.N. Coleman, Inkjet printing of silver nanowire networks. ACS Appl. Mater. Inter. **7**(17), 9254–9261 (2015)
40. M.A.U. Karim, S. Chung, E. Alon, V. Subramanian, Fully inkjet-printed stress-tolerant microelectromechanical Reed relays for large-area electronics. Adv. Electron. Mater. **2**(5), 1–8 (2016)
41. M. Gao, L. Li, Y. Song, J. Mater. Chem. C **5**, 2971–2993 (2017)
42. M.F. Farooqui, A. Shamim, Sci. Rep. **6**, 28949 (2016)
43. S. Ammu, V. Dua, S.R. Agnihotra, S.P. Surwade, A. Phulgirkar, S. Patel, S.K. Manohar, J. Am. Chem. Soc. **134**, 4553–4556 (2012)
44. B. Ando, S. Baglio, All-inkjet printed strain sensors. IEEE Sensors J. **13**, 4874–4879 (2013)
45. S. Cruz, D. Dias, J.C. Viana, L.A. Rocha, Inkjet printed pressure sensing platform for postural imbalance monitoring. IEEE Trans. Instrum. Meas. **64**(10), 2813–2820 (2015)
46. P. Giannakou, M.O. Tas, B. Le Borgne, M. Shkunov, Water-transferred, inkjet-printed supercapacitors toward conformal

and epidermal energy storage. ACS Appl. Mater. Interfaces. **12**(7), 8456–8465 (2020). https://doi.org/10.1021/acsami.9b21283

47. Szymon Sollami Delekta, Mikael Östling, Jiantong Li, Wet transfer of inkjet printed graphene for microsupercapacitors on arbitrary substrates. ACS Appl Energ Mater. **2**(1), 158–163 (2019). https://doi.org/10.1021/acsaem.8b01225
48. E. Sowade, K.Y. Mitra, E. Ramon, C. Martinez-Domingo, F. Villani, F. Loffredo, H.L. Gomes, R.R. Baumann, Up-scaling of the manufacturing of all-inkjet-printed organic thin-film transistors: device performance and manufacturing yield of transistor arrays. Org. Electron. **30**, 237–246 (2016). https://doi.org/10.1016/j.orgel.2015.12.018
49. S. Singh, Y. Takeda, H. Matsui, S. Tokito, Flexible inkjet-printed dual-gate organic thin film transistors and PMOS inverters: noise margin control by top gate. Org. Electron. **85**, 105847 (2020). https://doi.org/10.1016/j.orgel.2020.105847
50. M. Min, R.F. Hossain, N. Adhikari, A.B. Kaul, Inkjet-printed organohalide 2D layered perovskites for high-speed photodetectors on flexible polyimide substrates. ACS Appl. Mater. Interfaces. **12**(9), 10809–10819 (2020). https://doi.org/10.1021/acsami.9b21053
51. Lu. Zhou, L. Yang, Yu. Mengjie, Yi. Jiang, C.-F. Liu, W.-Y. Lai, W. Huang, Inkjet-printed small-molecule organic light-emitting diodes: halogen-free inks, printing optimization, and large-area patterning. ACS Appl. Mater. Interfaces. **9**(46), 40533–40540 (2017). https://doi.org/10.1021/acsami.7b13355
52. F. Villani, P. Vacca, G. Nenna, O. Valentino, G. Burrasca, T. Fasolino, C. Minarini, D. della Sala, Inkjet printed polymer layer on flexible substrate for OLED applications. J. Phys. Chem. C. **113**, 13398–13402 (2009). https://doi.org/10.1021/jp8095538
53. Z. Wang, H. Zhou, J. Lai, B. Yan, H. Liu, X. Jin, A. Ma, G. Zhang, W. Zhao, W. Chen, Extremely stretchable and electrically conductive hydrogels with dually synergistic networks for wearable strain sensors. J. Mater. Chem. C **6**, 9200–9207 (2018). https://doi.org/10.1039/c8tc02505c
54. J. Lai, H. Zhou, Z. Jin, S. Li, H. Liu, X. Jin, C. Luo, A. Ma, W. Chen, Highly stretchable, fatigue-resistant, electrically conductive, and temperature-tolerant ionogels for high-performance flexible sensors. ACS Appl. Mater. Interfaces **11**, 26412–26420 (2019). https://doi.org/10.1021/acsami.9b10146
55. Chang-Ge. Zhou, Wen-Jin. Sun, Li-Chuan. Jia, Xu. Ling, Kun Dai, Ding-Xiang. Yan, Zhong-Ming. Li, Highly stretchable and sensitive strain sensor with porous segregated conductive network. ACS Appl Mater Interfaces. **11**(40), 37094–37102 (2019). https://doi.org/10.1021/acsami.9b12504
56. M. Amjadi, K.U. Kyung, I. Park, M. Sitti, Stretchable, skin-mountable, and wearable strain sensors and their potential applications: a review. Adv. Funct. Mater. **26**, 1678–1698 (2016). https://doi.org/10.1002/adfm.201504755
57. J.H. Kim, J.Y. Hwang, H.R. Hwang, H.S. Kim, J.H. Lee, J.W. Seo, U.S. Shin, S.H. Lee, Simple and cost-effective method of highly conductive and elastic carbon nanotube/polydimethylsiloxane composite for wearable electronics. Sci. Rep. **8**, 1375 (2018). https://doi.org/10.1038/s41598-017-18209-w
58. T. Borca-Tasciuc, M. Mazumder, Y. Son, S.K. Pal, L.S. Schadler, P.M. Ajayan, Anisotropic thermal diffusivity characterization of aligned carbon nanotube-polymer composites. J. Nanosci. Nanotechnol. **7**, 1581–1588 (2007). https://doi.org/10.1166/jnn.2007.657
59. Y.R. Jeong, H. Park, S.W. Jin, S.Y. Hong, S.S. Lee, J.S. Ha, Highly stretchable and sensitive strain sensors using fragmentized graphene foam. Adv. Funct. Mater. **25**, 4228–4236 (2015). https://doi.org/10.1002/adfm.201501000
60. J.H. Kong, N.S. Jang, S.H. Kim, J.M. Kim, Simple and rapid micropatterning of conductive carbon composites and its application to elastic strain sensors. Carbon **77**, 199–207 (2014). https://doi.org/10.1016/j.carbon.2014.05.022
61. S.-H. Bae, Y. Lee, B.K. Sharma, H.-J. Lee, J.-H. Kim, J.-H. Ahn, Graphene-based transparent strain sensor. Carbon **51**, 236–242 (2013). https://doi.org/10.1016/j.carbon.2012.08.048
62. X. Wang, J. Sparkman, J. Gou, Strain sensing of printed carbon nanotube sensors on polyurethane substrate with spray deposition modelling. CompComm. **3**, 1–6 (2017)
63. H. Zhao, Y. Zhang, P.D. Bradford, Q. Zhou, Q. Jia, F.G. Yuan, Y. Zhu, Carbon nanotube yarn strain sensors. Nanotechnology. **21**, 305502 (2010)
64. S. Li, J.G. Park, S. Wang, R. Liang, C. Zhang, B. Wang, Working Mechanisms of Strain Sensors Utilizing Aligned Carbon Nanotube Network and Aerosol Jet Printed Electrodes. Carbon **73**, 303–309 (2014). https://doi.org/10.1016/j.carbon.2014.02.068
65. H. Lee, D. Lee, J. Hwang, D. Nam, C. Byeon, S.H. Ko, S. Lee, Silver nanoparticle piezoresistive sensors fabricated by roll-to-roll slot-die coating and laser direct writing. Opt. Express **22**, 8919–8927 (2014). https://doi.org/10.1364/oe.22.008919
66. B. Thompson, H.S. Yoon, Aerosol-printed strain sensor using PEDOT: PSS. IEEE Sens. J. **13**, 4256–4263 (2013). https://doi.org/10.1109/jsen.2013.2264482
67. M.Q. Le, F. Ganet, D. Audigier, J.F. Capsal, P.J. Cotttinet, Printing of microstructure strain sensor for structural health monitoring. Appl. Phys. A. https://doi.org/10.1007/s00339-017-0970-x (2017).

68. J. Park, D. Nam, S. Park, D. Lee, Fabrication of flexible strain sensors via roll-to-roll gravure printing of silver ink. Smart Mater Struct. **27**, 085014 (2018). https://doi.org/10.1088/1361-665X/aacbb8
69. S. Gong, W. Schwalb, Y.W. Wang, Y. Chen, Y. Tang, J. Si, B. Shirinzadeh, W.L. Cheng, A wearable and highly sensitive pressure sensor with ultrathin gold nanowires. Nat. Commun. **5**, 3132 (2014)
70. J. Lee, S. Kim, J. Lee, D. Yang, B.C. Park, S. Ryu, I. Park, A stretchable strain sensor based on a metal nanoparticle thin film for human motion detection. Nanoscale **6**, 11932 (2014)
71. K.K. Kim, S. Hong, H.M. Cho, J. Lee, Y.D. Suh, J. Ham, S.H. Ko, Highly sensitive and stretchable multidimensional strain sensor with prestrained anisotropic metal nanowire percolation networks. Nano Lett. **15**, 5240 (2015)
72. J. Eom, J.S. Heo, M. Kim, J.H. Lee, S.K. Park, Y.H. Kim, Highly sensitive textile-based strain sensors using poly (3, 4-ethylenedioxythiophene): polystyrene sulfonate/silver nanowire-coated nylon threads with poly-L-lysine surface modification. RSC Adv **7**(84), 53373–53378 (2017)
73. C. Pang, G.Y. Lee, Ti. Kim et al., A flexible and highly sensitive strain-gauge sensor using reversible interlocking of nanofibers. Nat Mater **11**, 795–801 (2012)

Publisher's Note Springer Nature remains neutral with regard to jurisdictional claims in published maps and institutional affiliations.